

Search for free quarks produced at 800 GeV/c using a new concentration technique

H. S. Matis and H. G. Pugh

Nuclear Science Division, Lawrence Berkeley Laboratory, 1 Cyclotron Road, Berkeley, California 94720

R. W. Bland, D. H. Calloway, S. Dickson, C. L. Hodges, D. Joyce, M. A. Lindgren,
T. L. Palmer, M. L. Savage, and A. B. Steiner

Physics and Astronomy Department, San Francisco State University, San Francisco, California 94132

A. A. Hahn and G. L. Shaw

Physics Department, University of California at Irvine, Irvine, California 92717

R. Tokarek

Fermi National Accelerator Laboratory, Batavia, Illinois 60510

R. Slansky

Los Alamos National Laboratory, Los Alamos, New Mexico 87545

(Received 1 September 1988)

A high-sensitivity experiment was performed to detect free quarks produced in collisions of 800-GeV/c protons with a heavy target at Fermilab. Two quite different, high-concentration methods were used to obtain a small drop of Hg containing any produced quarks which stopped in a large amount of material. Using a new technique, secondaries were stopped in Hg tanks and the Hg was then distilled to small drops. In a second method, secondaries were stopped in liquid-nitrogen tanks, and charged atoms were collected electrostatically on Au-coated electrodes. The Au coatings were dissolved in Hg. The Hg drops from both techniques were then tested for quarks in the San Francisco State University automated Millikan apparatus. These results show that charged $\frac{1}{3}$ quarks are produced below levels of 1.2×10^{-10} at 90% C.L. for both methods. Upper limits are also presented for charged $\frac{2}{3}$ quarks. The distillation technique should prove useful in performing high-sensitivity quark searches in future beam-dump experiments.

I. INTRODUCTION

The San Francisco State University (SFSU) automated Millikan drop apparatus provides a well-established method for testing bulk Hg for free quarks. It has been successfully used in high-sensitivity searches¹⁻³ for quarks produced at accelerators and for quarks trapped inside bulk matter. This procedure complements direct counter experiments which look for quarks produced at accelerators. We present here the results of an experiment (E747) at Fermilab which searched for free quarks produced at the Tevatron in 800-GeV/c proton collisions with heavy target nuclei. In addition to an electrostatic concentration scheme which has been described in several publications, we describe a new high-concentration method which involves the distillation of Hg from tanks which have stopped secondary particles. Only one particle which could be interpreted as a fractionally charged particle was found. However, its production rate is consistent with known background. Therefore, no evidence of fractional charge can be found. Preliminary results⁴ from this experiment have been discussed.

As there is impressive experimental evidence and theoretical bias against the existence of free quarks,^{5,6}

most particle physicists have accepted the idea of quark confinement within QCD. Nevertheless, the only proof on confinement is the fact that free quarks have not yet been observed. New high-sensitivity experiments must be done when appropriate new opportunities arise, such as the commissioning of a new accelerator where a new threshold could be passed. Clearly, the consequences of finding free quarks would be of immense importance.

Theoretically, it is widely believed that unbroken non-Abelian gauge theories confine the charges of the local symmetry group. However, it is not possible to determine definitely from present theoretical and experimental results if the exact local symmetry in nature is $SU(3)_{\text{color}} \times U(1)_{\text{em}}$. If this theory is exact, color is confined and, consequently, no free quarks can be produced. Models have been produced in which $SU(3)_{\text{color}}$ is spontaneously broken and color is not an exact local gauge symmetry. Here free quarks could be produced in certain experiments and yet not violate the present experimental constraints. In fact, it was suggested that the production of free fractional charge might be greatly enhanced in relativistic heavy-ion collisions as compared to elementary-particle collisions.^{7,8} The environment of a quark-gluon sea created in the heavy-ion collision would enhance the separation of a particle with fractional

charge from the remaining colored fragment by maximizing the quark density that can be achieved. It might be possible to create a similar environment with large- A nuclei in proton-nucleus collisions.

The signature of a quark produced at an accelerator may be very different from that of a typical hadron. De Rújula, Giles, and Jaffe argued⁷ that after a quark is produced it would capture nucleons as it passes through a detector. Since a bare quark could have a net color charge, its interaction with matter could be significantly stronger than a typical hadron. Therefore, its signature could be a particle with varying electric charge-to-mass ratio. Such characteristics are very difficult to detect with conventional detectors, so many previous accelerator or cosmic-ray experiments would have missed such a signature. In addition, refined material, which has been used in many bulk-matter experiments, might have been depleted of its original quark content during its production process.⁹

The SFSU apparatus can detect free quarks with charge of $|\frac{4}{3}|e$ in addition to $|\frac{1}{3}|e$ or $|\frac{2}{3}|e$, where e is the charge of an electron. In fact, any fractionally charged particle can be measured, as long as its residual charge, the deviation from integral charge, is outside the resolution for measuring integral charge. Thus, exotic objects such as hadronic color singlets and leptoquarks can be detected. However, as we have assumed in our Monte Carlo calculations that quarks stop via the strong interaction, the quoted limits must be modified for exotic processes which have much weaker quark-nucleon couplings.

In this paper we define free quarks as any strongly interacting fractionally charged particle. Charges are measured in units of e .

II. EXPERIMENTAL DESIGN

As Fermilab entered a new fixed-target energy regime with its 800-GeV/ c Tevatron program, our collaboration undertook a quark-search experiment to explore this region with a high-statistics proton-nucleus experiment. Experiments^{10,11} have been done for $p\bar{p}$ collisions at the higher energy of the CERN SPS collider with much less sensitivity than can be done with our method.

This experiment was designed to avoid problems that many quark-search experiments have had by using bulk matter to capture any produced quark independent of the details of the production mechanism. Bulk matter has the additional advantage that essentially the full intensity of an accelerator can be directed into the targets. Since quarks are stable because of charge conservation, the analysis of the stopping material, including the target, can be done later in a laboratory.

III. SEARCH FOR QUARKS TRAPPED IN MERCURY

Our experiment consists of four stages: (1) production of secondaries in collisions of the beam with heavy target nuclei; (2) stopping of the secondaries in tanks of liquid Hg; (3) concentrating any stopped quarks into a small (about 10 mg) drop of Hg; and (4) testing this Hg drop for quarks using the SFSU Millikan apparatus.

Four steel cylinders filled with mercury were centered in an 800-GeV/ c primary proton beam line. The integrated intensity was 1.0×10^{15} protons on target. Each cylinder, whose diameter was 16 cm and length was 10 cm, contained 1.50 liters of mercury. The tanks were filled almost to the top with Hg. An air gap of about 4 cm was left to allow for expansion of the liquid due to beam heating. The geometrical arrangement is shown in Fig. 1. In order to sample different depths of the hadronic shower, 10 cm of lead were interspersed between each of the mercury targets to slow any produced quarks.

The exposure to the beam lasted for 2.5 weeks. The temperature was monitored for each of the tanks. The highest temperature reached was 56.7°C for the first tank when the beam intensity was about 3×10^{11} for a spill which occurred once every 60 sec. The temperatures of the other tanks decreased monotonically. The temperature of the last tank was significantly over the room value. After the exposure, the steel tanks were monitored by measuring the radioactivity of the steel to confirm that the beam hit the tanks in the center.

As the SFSU Millikan apparatus can only measure material whose mass is of order milligrams, it is necessary to concentrate any quarks in the original volume of mercury to a much smaller volume. We decided that the best way is to use distillation apparatus to concentrate the exposed mercury.

The most significant argument for quarks remaining in the residue when Hg is heated is that a "quarked" atom will be attracted to its neighboring atoms through its image charge.⁹ The quarked atom cannot be neutralized by other integrally charged atoms. The attraction of the image charge holds the quarked atom within the sample of Hg when the sample is gently heated during the process of distillation, as long as the kinetic energy of the atoms are less than the binding energy of the image charge. Thus, while the Hg is heated, the normal atoms of Hg will escape, leaving the fractionally charged atoms in the liquid.

A more speculative argument can be made using the chemistry of the quarked nucleus. Lackner and Zweig¹² have shown that when a quark attaches itself to a nucleus the new atom will have different chemical properties.

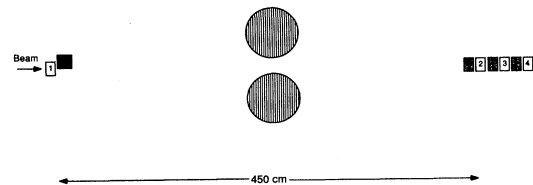


FIG. 1. Top view of the experiment for irradiating the Hg tanks. A number refers to the Hg tank label to which it is referred in the text. The shaded rectangles are Pb attenuators which were used to slow down quarks. The striped circles represent a cylindrical container which was filled with freon-113.

The difference can be viewed as a translation of the chemical properties in the periodic table. They have calculated new electronegativities for quarked atoms and identified the closest element that has a similar value. For instance, if a $-\frac{1}{3}$ quark is captured by a Hg atom it will behave like a Cd atom while a $-\frac{2}{3}$ quark would change a Hg atom to behave like a Sr atom. Since all of the neighbors of mercury and most of the other elements have much higher boiling points, the chemical shift would result in the quarked atom that has a much lower vapor pressure and therefore would stay in the residue when heated. Therefore, from all of these arguments, we conclude that heating the mixture of mercury and quarked atoms should selectively remove the mercury atoms from the sample and leave the quarked atoms in the residue.

Because of the high radioactivity of the Hg, distillation was not started until 12 months after the exposure. First, approximately 700 ml of Hg was transferred to the distillation still and then slowly heated to about 300°C under vacuum. When the residue was reduced to a volume of 15 ml, the heat was removed. After a short time, the residue was transferred to a smaller distillation flask. Using the same procedure, the residue was heated until a few milligrams of material was left. During this procedure, the Hg was held well below the point where it would boil. This residue was later examined in the SFSU Millikan apparatus.

The mercury in the four tanks was distilled by a factor of 3.3×10^6 , 4.0×10^6 , 6.0×10^3 , and 3.91×10^5 , respectively. The reason for the large difference in the distillation factor between the tanks was due to the different purity of the original samples and the desire to measure at different concentration levels. In addition, some undistilled mercury was measured for trapped quarks.

A. Tests of distillation procedure

The concentration of fractional charged objects in the mercury distillate compared to the undistilled mercury has been estimated from four different measurements: (1) mass concentration, (2) γ spectrum measurements using a GeLi detector, (3) γ -ray spectrum measurements from a NaI detector, and (4) specific activity measurements. These tests are designed to measure the concentration due to the distillation process and the amount of quarks lost to the distillate.

The first method, which is straightforward, was designed to measure the concentration efficiency of the distillation procedure. The mass of the initial undistilled samples (typically a few kilograms) and the mass of the final residue (typically a few milligrams) were measured. Assuming that no fractional charges are lost in the distillation, the ratio of the mass of the initial sample to the mass of the residue is the concentration.

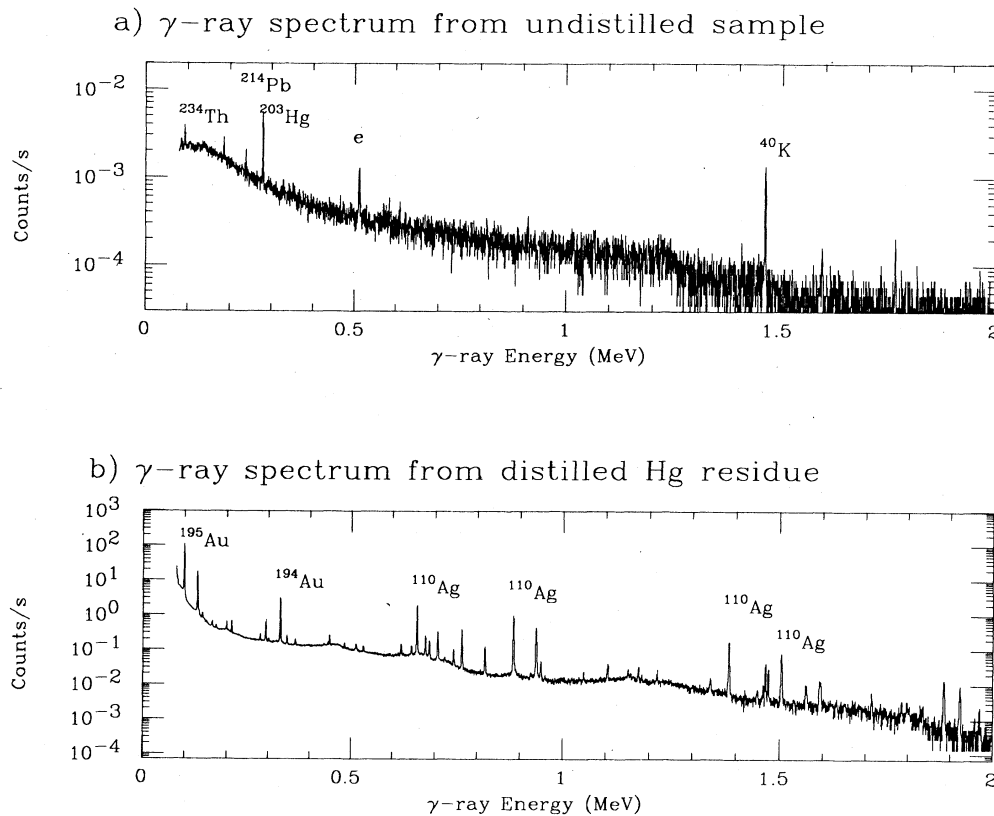
Method (2), as well as methods (3) and (4), has a critical assumption that the quarked atoms distill similar to the radioactive metallic contaminants, such as Au and Ag, which are produced by the bombardment of the mercury by the proton beam. The radioactive decay of the metallic contaminants is used to measure the concentrations in

the undistilled and distilled samples. By measuring the ratio of the elements in these two samples, we can calculate the efficiency of the distillation for keeping quarks in the residue. This method measures the amount of quarks which remain in the residue.

To perform this test, a GeLi detector was used to measure the γ spectrum from both the undistilled Hg and the residue. Figure 2 shows these two measurements from the distillation of tank 2. The γ -ray lines were measured for the residue and for a similarly sized drop from the undistilled Hg. In the undistilled sample, ^{203}Hg , which was created by the proton beam, and room background isotopes such as ^{40}K , ^{214}Pb , and ^{236}Ra , which were produced by radiation from impurities in the detector or from the adjacent environment, can be identified. However, the residue contained significant quantities of ^{194}Au , ^{195}Au , and ^{110}Ag . These elements could be measured in the residue as they were concentrated during the distillation procedure. An upper limit for the concentration of ^{195}Au in the distillation was estimated by comparing the number of counts in the residue produced by the decay of ^{195}Au to the maximum plausible number of counts above background in the undistilled sample. From these data, we can estimate that ^{195}Au was concentrated by a factor greater than 4.2×10^5 . The volumetric measurement for the sample used in method (1) was 4.0×10^6 and therefore the efficiency for retaining quarks in the residue measured by method (2) is better than 10%.

Method (3) used a NaI spectrometer to identify the ratio of the amount of metallic contaminants to Hg in the distillate and the residue. The purpose of this method is to identify the fraction of quarks which did not remain in the residue. A NaI spectrometer was used to identify ^{203}Hg through its β decay to ^{203}Tl from its characteristic γ ray in both samples. Several x rays and low-energy γ rays, assumed to be from Au and the other metallic contaminants, were observed in the residue. By comparing the ratio of the number of counts due to metallic contaminants in the distillate, the residue, and the undistilled Hg, we calculate that over 80% of the Au in the original sample was transferred to the residue.

In method (4), the total activity of similar mass samples of undistilled, distillate, and residue are measured. This procedure is complementary to method (3) as its purpose is to measure the efficiency for trapping quarks in the residue. The specific activity was simply measured by counting the number of radioactive decays of very small equally sized Hg samples using a NaI detector. The concentration of the distillate was assumed to be entirely due to ^{203}Hg and background. Then the impurity activity in the undistilled sample was found by subtracting the distillate activity from the measured activity. The impurity activity of the residue was found using a similar procedure. Then, the ratio of the impurity residue activity to the impurity undistilled activity was compared to the volumetric ratio [method (1)]. This ratio was measured for two distillations and was found to be 52% and 57%, indicating that only about 50% of the gold was retained in the residue. This measurement of efficiency of keeping the quarks in the residue is lower than the value measured in method (3). To be conservative, we will use



50% as our estimate of the number of quarks that remain in the distillation residue.

Thus, we consider a reasonable estimate on the efficiency of concentrating fractional charges to be 50% of the distillation factor measured by method (1). This value is included in the upper-limit calculation.

B. Analysis of residue from distillation

Once the Hg was concentrated, it was tested in a Millikan-type apparatus which has been described in our previous publications.¹⁻⁴ Figure 3 shows a schematic of the apparatus. Hg drops are made by a piezoelectrically driven dropper (a). A drop falls between two electrically charged, horizontal plates (b). The image of the drop is illuminated by a laser (c) and projected on a screen of horizontal slits (e). A photomultiplier (f) detects light which passes through the screen. The signal from the photomultiplier is digitized by the computer.

The velocity of the drop can be calculated by measuring the time that the photomultiplier detects peaks of lights among adjacent slits. By measuring the terminal velocity and using Stokes's law, one can calculate the radius. The polarity of the electric field is switched two

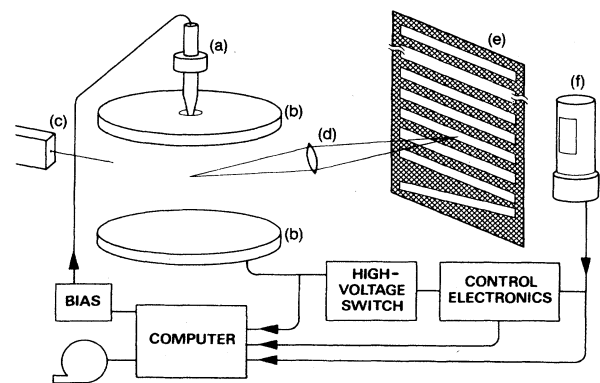


FIG. 3. Schematic of the SFSU Millikan apparatus. Shown in this figure is (a) the Hg dropper which ejects drops into two electrically charge parallel plates (b). A laser (c) produces light which illuminates a Hg drop. The image is focused using a telescope (d) on a vertical screen of horizontal slits (e). The light is detected by a photomultiplier (f), whose output signal is recorded by a computer.

times while the drop passes through the plates. By measuring the change in terminal velocity in the regions of different electric charge, the net charge of the drop can be measured. By comparing the velocity of the drop before the first electrical field reversal and after the second reversal, it can be determined whether there was a charge change on the drop during a measurement. Careful analysis of the velocity profile is used to avoid inclusion of possible incomplete measurements such as multiple drops and double charge changes.

Figure 4 shows a fitted residual-velocity curve that was measured from a typical drop. The velocity is fitted in the three different regions shown on that curve. The curve shows the difference between the fitted and the measured velocity. In the first region, the drop falls and reaches terminal velocity. The first arrow shows when the sign of the electric field is reversed. After a short time, the drop again reaches its terminal velocity. At the second arrow the field is again reversed. After passing a few more slits, it reaches its terminal velocity. For this particular drop the measured charge was $19e$. The net charge resolution for the apparatus was measured to be about $0.04e$ for these series of runs. The total mass of mercury processed before this experiment was run is of the order of milligrams.

From the mercury tested, a total of a $230 \mu\text{g}$ of Hg from the third tank, $47.3 \mu\text{g}$ of Hg from the fourth tank, and $5.6 \mu\text{g}$ from the first tank passed all tests. These tests included checks for charge changing, multiple drops, and good χ^2 for fits to the velocity. A total of 65 713 drops passed these preliminary on-line and off-line cuts. From this sample there were five events that had a significant residual fractional charge.

In order to determine whether an event is truly a fractionally charged particle, the characteristics of it were carefully compared to other events measured at approximately the same time. The most sensitive test for trajec-

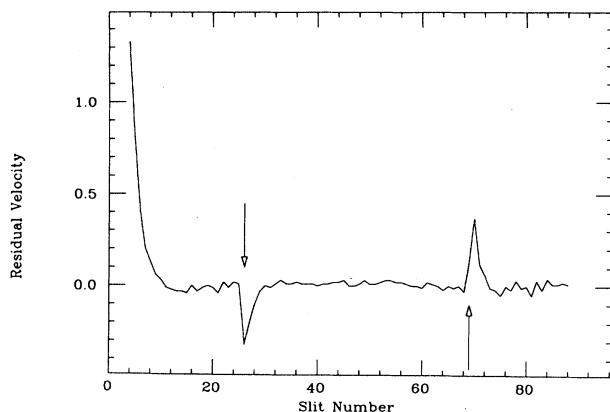


FIG. 4. The measured velocity minus the fitted velocity is shown for a typical drop. The unit of velocity is arbitrary. The arrows indicate the location of the drop when the field was reversed. In this figure the fitted velocity was fitted independently in each of the three regions. There was no term which described the region where the field was changing.

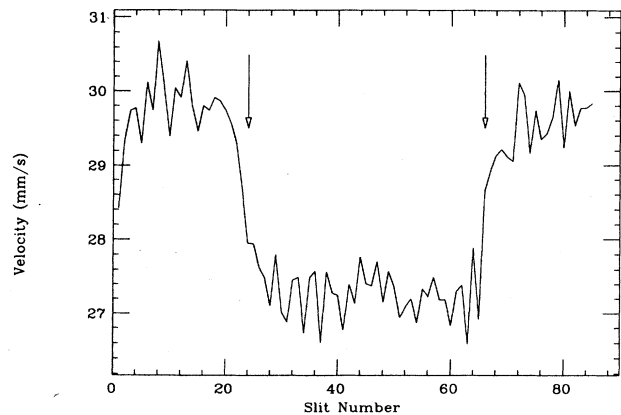


FIG. 5. The velocity distribution of the drop R0 710 039.203. The two arrows show the location where the field was changed.

tory errors is to examine the deviation from the average of the residuals from a fit to linear velocity plus an exponential velocity term when the field is changed. From this information, we can then determine the residual between fit and data. The residuals of all events that have a measured fractional charge are examined with the average distribution for charged drops whose charge is very close to the event in question.

Figure 5 shows the velocity distribution for one, R0 710 039.203, of the five candidate drops with fractional charge. The notation R0 710 039.203 indicates that this drop was drop number 203 in run 710 039. To make a more detailed analysis, it is necessary to examine the deviation from the average residual for this drop, which is displayed in Fig. 6. The average residual is the deviation from the best fit to the trajectory of the drop, which

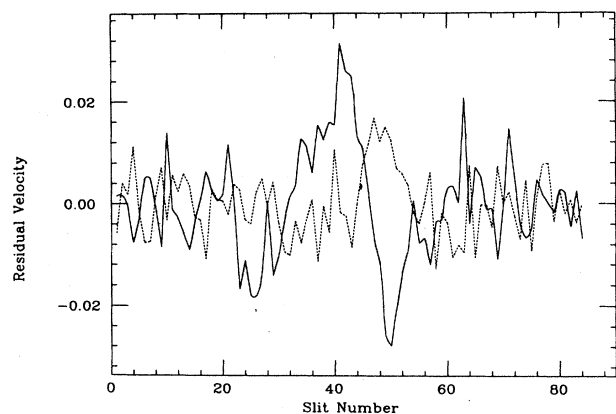


FIG. 6. The solid line shows the difference between the measured and fitted velocity for drop R0 710 039.203. A similar curve for a measurement with nearly identical charge is shown as a dashed line. For this plot, an exponential curve was used to parametrize the region where the electric field changed.

is measured at each slit. Also on this figure is the residual plot for an integrally charged drop that had almost the same charge that was measured in the same run. Notice the significant deviation in R0 710 039.203 around slit 45. The reduced χ^2 of the deviation of the residual for this event (2.25), which is shown in Fig. 7, is more than three standard deviations higher than the average event (1.0 ± 0.4). Because of its significant deviation from the average residual, this event is rejected from the final analysis data set.

Similarly, another event can be rejected as its radius is significantly different from the neighboring events. Finally, we arrive at three fractionally charged candidate drops that pass all tests. The residual charge of all drops that passed these final tests is shown in Fig. 8. Two of the events near $\frac{1}{3}e$ were subsequently identified as a "test quark." "Test quarks" are events that have their charge displaced randomly by either $\pm\frac{1}{3}e$ or by $\pm re$ by the data acquisition computer. The variable r is a positive number less than 1. These test quarks are generated so that we can measure the efficiency of the analysis procedure in detecting quarks. These two events were the only test events that were generated and therefore the detection efficiency for quarks is 100%. Because of these small statistics, we take the value of 80% which is derived from this and previous runs.

At this stage in the analysis, one candidate for fractional charge, R0 710 052.322, remained near residual charge $\frac{1}{2}$. Event R07 100 052.322 showed no evidence for anomalous deviation from the average residual (χ^2 is 1.3). However, this drop is from a sample of very high concentration and radioactivity and consequently the run contained numerous charge changes. In fact, one drop in five was rejected as a charge change by examining the difference between its initial and final velocities. The apparatus is sensitive to a charge change over about 60 slits. However, the probability of a charge change at one field reversal and an equal and opposite charge at the other reversal is significant. In fact, if a change occurs within

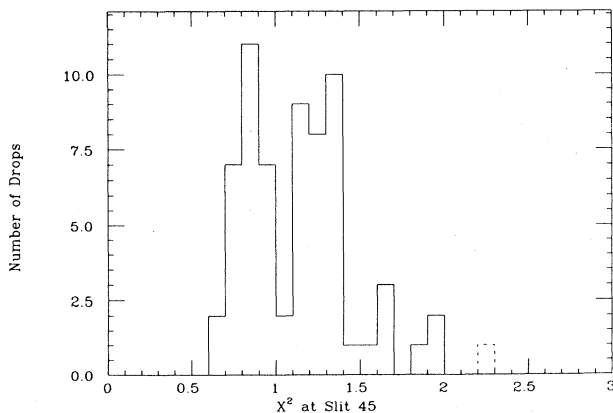


FIG. 7. Histogram of the χ^2 distribution for drops that have closely measured charge to event R0 710 039.203 from the same run and three nearby runs. The dashed line shows the χ^2 for event R0 710 039.203.

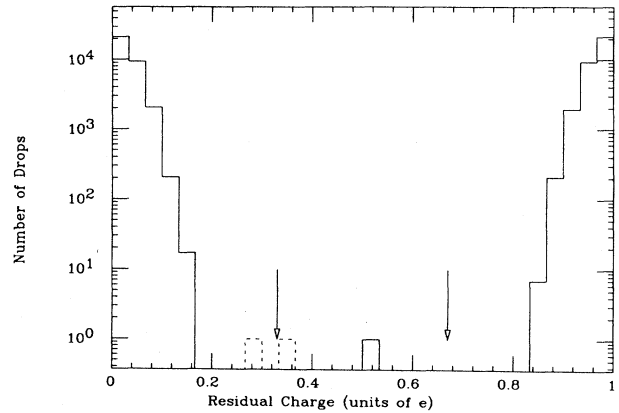


FIG. 8. A histogram of the measured residual charge for drops which passed all acceptance tests for the distilled Hg. The two arrows show the expected position for residual charge for any drop which contains a charged $\frac{1}{3}$ or $\frac{2}{3}$ quark. The one event at residual charge $\frac{1}{2}$ can be explained as a background event. The other two events, which are indicated by dashed lines, are test events generated by the data acquisition computer.

three slits of the field switch then such a change cannot be detected. The probability of such a change is then $(\frac{1}{3})(\frac{3}{60})(\frac{1}{3})(\frac{3}{60})(\frac{1}{2})$ or $(\frac{1}{20000})$. We have measured a total 12 000 drops and thus have about 50% chance of having a double opposite charge change around the field switches.

Furthermore, Monte Carlo studies have shown that opposite charge changes of one unit at the time of field switching produce data which when reconstructed appear to have a fractional charge of $0.50e \pm 0.05e$. The fact that the reconstruction algorithm assumes that the drop's charge does not vary during the time of measurement leads to an incorrect measurement of charge whenever there is a charge change.

Thus, although event R07 100 052.322 cannot be rejected using our usual criteria, the measurement of a fractional charge for that event is consistent with the most likely hypothesis that an opposite charge change happened. Consequently, we conclude that this event is probably produced by a double charge change on an integrally charged drop and should not be identified as containing a fractionally charged particle.

C. Monte Carlo calculation of quark stopping

An estimate of the bound on the inclusive quark production rate requires a model for quark production, and a model for hadronic quark scattering. The Bethe-Bloch formula¹³ is adequate for estimating the energy loss from the electromagnetic interactions of a fractional charge. We have written a Monte Carlo program to estimate the efficiency of the tanks to stop a produced quark, and varied several parameters of a model for quark production and scattering over a reasonable range of values. These calculations should be good enough to estimate the

bounds of the production cross section of fractional charge within an order of magnitude.

The first step of the calculation is to determine by Monte Carlo simulation where the primary beam-target collision occurs in the apparatus. We compute the mean free path for the incoming proton beam using, as the inelastic cross section,¹⁴

$$\sigma_{\text{inel}} = 7.8(A_p^{1/3} + A_t^{1/3} - 0.9)^2 \text{ mb}, \quad (1)$$

where A_p is the number of nucleons in the projectile and A_t is the number in the target. When an interaction occurs, quarks are produced. Only one of these quarks per interaction is followed in the Monte Carlo simulation.

If quarks are produced in high-energy collisions, it is reasonable to assume the collision is central and to use a standard hadronic interaction¹⁵ model. Thus, we assume an isotropic inclusive quark distribution in the center-of-mass frame of the beam and target nucleus. As only a fraction of the target nucleons could be involved in this collision, we define an "effective" target mass in defining the center of mass. The effective mass of the target nucleus is one of the parameters that are varied.

We select an exponential distribution for the quark produced in the proton-nucleus collision. This distribution has a high tail, in order to be conservative about the angular distribution of the produced quark. For simplicity of calculation, we select the distribution in the center-of-mass frame,

$$N(k)d^3k/\sqrt{2E} = \exp(-\sqrt{8}k/\langle k_T^2 \rangle^{1/2})k^2 dk d\Omega, \quad (2)$$

where $\langle k_T^2 \rangle^{1/2}$ is the rms value of the transverse momen-

tum in GeV/c, E is the energy of the quark, and k is the magnitude of the three-momentum in the c.m. frame, also in GeV/c.

From Eq. (2), we obtain the momentum and direction of the quark in this frame, which we then Lorentz transform to the laboratory frame. The quark propagates in a straight line through the various elements of the primary target and collection apparatus until it either scatters by its strong interactions, losing a fraction of its laboratory energy, or it slows down electromagnetically by energy loss according to the Bethe-Bloch formula. When the velocity of the particle reaches 0.03c, the lower limit for validity of the Bethe-Bloch formula, the quark is stopped and then captured by a nucleus.

The hadronic interactions of the quark are also assumed to be central with the distribution used in Eq. (2). Of course, it might be expected that quarks have a cross section for scattering peripherally but such contributions were neglected. The mean free path for a quark-nucleon interaction is defined by a third parameter σ_q , which is the quark-nucleon total inelastic cross section. Typically, we assume σ_q is 5 or 20 mb/nucleon in the target and ignore nuclear shadowing. These parameters can be rescaled, if it is assumed the cross section goes as $A^{2/3}$. For example, 5 and 20 mb should be replaced by 29 and 117 mb/nucleon for Hg and by 12 and 48 mb/nucleon for interactions with N_2 .

It is necessary to define the center of mass for the quark-nucleus scattering, so we must assume a quark mass and again an effective target mass. We have taken a variety of quark masses: 1, 5, and 10 GeV. The calculations have been carried out for two values of $\langle k_T^2 \rangle^{1/2}$ at 0.5 and 2.0 GeV/c. Table I shows the probability for

TABLE I. Fraction of quarks which stop in Pb tanks.

Effective target mass (GeV)	Quark-nucleus cross section (mb)	Tank	Fraction of quarks stopped with mass		
			1 GeV	5 GeV	10 GeV
1	5	1	0.000	0.000	0.005
		2	0.015	0.017	0.029
		3	0.019	0.052	0.044
		4	0.018	0.062	0.064
4	5	1	0.006	0.013	0.006
		2	0.009	0.032	0.044
		3	0.007	0.043	0.046
		4	0.010	0.052	0.064
10	5	1	0.011	0.017	0.010
		2	0.013	0.039	0.038
		3	0.005	0.028	0.060
		4	0.008	0.043	0.053
1	20	1	0.036	0.030	0.035
		2	0.038	0.100	0.129
		3	0.034	0.075	0.092
		4	0.014	0.028	0.020
4	20	1	0.068	0.054	0.033
		2	0.034	0.095	0.109
		3	0.026	0.058	0.079
		4	0.006	0.022	0.019
10	20	1	0.065	0.067	0.044
		2	0.026	0.088	0.089
		3	0.020	0.049	0.058
		4	0.003	0.016	0.026

quark stopping for several of these assumptions (the quark charge is $\frac{1}{3}$ and $\langle k_T^2 \rangle^{1/2}$ is 0.5 GeV/c). This experiment is sensitive to lighter-quark masses than the one shown in the table and to heavier masses as long as there is enough energy in the center-of-mass frame. Absorption probabilities for parameters that are not shown can be estimated by extrapolating the values in this table. For the purposes of calculating an upper limit, we chose the values for a cross section of 20 mb and a mass 1 GeV. A quark charge of $\frac{1}{3}$ has an absorption probability of 0.036, 0.038, 0.034, and 0.014 for the four tanks, respectively, while a quark charge of $\frac{2}{3}$ gives an absorption probability of 0.040, 0.054, 0.029, and 0.017.

If the charge were higher than the assumed $\frac{1}{3}e$, then quarks would be slowed down faster and thus more quarks would be stopped. Changing the charge to $\frac{2}{3}$ results in a stopping fraction of quarks of only a little more than the $\frac{1}{3}$ quark values. This factor is much less than the factor of 4 which would come if the Z^2 electromagnetic stopping is the most significant process. Consequently, the hadronic inelastic cross section is the dominant mechanism in this model.

From these data, an upper limit at 90% confidence level for $\frac{1}{3}$ charged-quark production from 800-GeV/c protons can be set at 1.7×10^{-10} quarks per incident proton for the first tank, 24.8×10^{-10} for the third tank, and 4.5×10^{-10} for the last tank. Combining the data from the tanks yields an upper limit of 1.2×10^{-10} . The limit for $\frac{2}{3}$ -charged quarks is 1.1×10^{-10} . Using the numbers in Table I, one can scale these limits for other assumptions on quark-nucleon interactions.

The nominal values for the parametrization of the quark-nucleus interaction that we choose to use in the acceptance are very conservative. As a quark would have a bare color charge, the strength of the interaction may be much stronger than a nucleon-nucleon interaction and consequently the calculated upper limits should be much tighter than are quoted in this paper. For instance, in the model⁷ of De Rújula, Giles, and Jaffe where quarks have an extremely large interaction, our limits would be at least an order of magnitude more sensitive.

IV. SECOND METHOD—TRAPPING QUARKS IN LN₂

A complementary method to trapping quarks in mercury was used in a second run. This method has been described in several publications. In a previous experiment,² CCl₄ was used to slow any produced quark and a charged fiber was used to trap it. For the present experiment because of the safety problems with handling CCl₄, it was initially decided to use a simpler and less dangerous polar liquid. At first, freon-113 (CCl₂FCClF₂) was chosen. However, chemicals (most probably related to H and F ions from disassociating freon atoms during the run) were produced which dissolved the quartz fibers. The next choice was to use liquid N₂ in insulated tanks.

The principal idea behind this method is that once a quark stops, it becomes captured by a neighboring nucleus. The resulting quarked atom is electrically charged and cannot be neutralized by the surrounding, integrally charged atoms. Consequently, the quarked atom will be

attracted to one of the charged wires. After the quarked atom reaches the wire, it will be trapped on the surface of the wire through its image charge.

In this run, the proton beam struck a 10-cm-thick lead target. A quark, produced in the interaction, could stop in one of the four nitrogen tanks whose layout is shown in Fig. 9. Each tank was constructed of 6.4-cm-thick polystyrene foam with a stainless-steel tank in the center. The dimensions of the steel tank were 46 cm \times 20 cm in the horizontal direction and 37 cm in the vertical direction. Two charged wires were placed in each tank. These wires, which consisted of a 125- μ m quartz fiber surrounded by about a 200- Å layer of Au, were held at potentials of 5000 and -5000 kV while the outer steel tank was held at ground potential.

The field configuration was selected to allow a collecting time on the order of minutes for N₂ atoms with a residual charge of $\frac{1}{3}$. In laboratory tests, we could see macroscopic particles drifting toward the electrodes, while presumably neutral particles remained stationary. So, the effect of collective motion of the liquid resulting from electroconvection¹⁶ does not reduce the collection efficiency of the electrodes.

The tanks were filled to within 2.5 cm of the top of the steel container and the voltage turned onto the wires about 2.5 h before the first beam particles struck the detector. The exposure lasted for 6.0 h with a total flux of 4.1×10^{13} 800-GeV/c protons on target. After waiting 1.5 h, the voltage was disconnected and the wires were removed from the LN₂. The LN₂ level dropped a total of 13 cm. About 3 cm can be attributed to energy deposited by the beam; while the rest of the loss can be attributed to evaporation caused by heat from the environment.

Immediately after the exposure, the wires were removed from their holders and then moved through a small bead of mercury, so that the Au containing any trapped quarks was transferred to the Hg bead. A total of four beads were used, so that each bead contained the residue from two wires. Measurements, at the time of the extraction, showed that the wires were significantly more radioactive than the surrounding material. When the wires were rinsed, the radioactivity was transferred to the Hg. As the radioactivity of the bead was sufficiently higher than the surrounding material, the ability to attract particles was demonstrated. Furthermore, visual observation of the wires under a microscope showed that more than 95% of the Au on the wire was transferred to Hg. Folding in the field configuration of the tanks, the

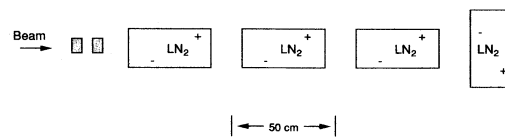


FIG. 9. Arrangement of liquid-N₂ tanks for the second phase of the experiment. Each tank contains two wires which were held at opposite high voltage. Each stainless-steel tank was held at ground potential.

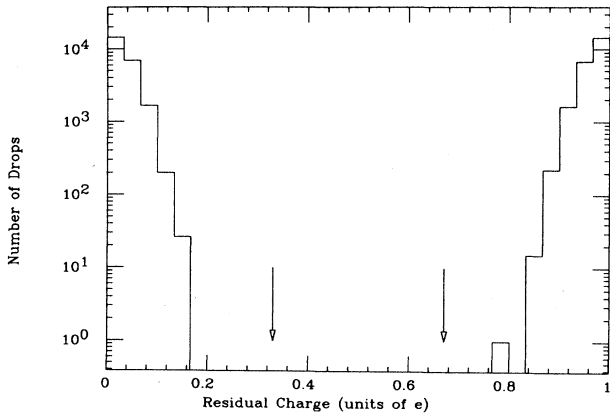


FIG. 10. A histogram of residual charge for drops for the liquid-N₂ data set which passed all acceptance tests. The two arrows show the expected position for residual charge for any drop which contains a charged $\frac{1}{3}$ or $\frac{2}{3}$ quark.

efficiency of this process to capture and trap charged particles can be estimated to be about 50%.

Measurements¹⁷ on trapping of charged atoms on a metallic surface have been done at University of California, Irvine (UCI) for a check of a double- β decay experiment¹⁸ by observing the decay of daughters of ^{222}Rn . This chain was introduced into the gas volume of a time-projection chamber (TPC) through the α decay of a ^{222}Rn atom to ^{218}Po . The ^{218}Po atoms, which are most probably positively charged, became attached to an aluminized Mylar surface which was held at -1 kV. The captured ^{218}Po decays to ^{214}Pb via α -particle emission. Then, the ^{214}Pb nucleus ($t_{1/2}=26.8$ m) decays by emitting an electron to ^{214}Bi ($t_{1/2}=19.7$ m) which also decays via emission of a β particle.

The UCI group found using their TPC that the efficiency to detect both the ^{214}Pb and ^{214}Bi decay at the same location was greater than 90%. Accounting for the misidentification probability of detecting the first decay and the efficiency to detect the second, they believe that their data are consistent for 100% trapping of the ^{214}Bi nuclei for a time scale of at least an hour. These results reinforce the hypothesis that once a quarked atom sticks on a wire, it becomes trapped.

A. Analysis of Hg beads

The four Hg beads were brought to the SFSU Millikan apparatus to determine, whether any fractional charge was captured using the same procedure to look for quarks that was previously described in this paper. The Hg beads were combined and half of this mixture was diluted in triple distilled Hg to make a sample of 7.0 mg. It was necessary to dilute the sample in order that the sample could be inserted safely in the Hg dropper. From that amount, about 213 μg of material were processed. The charge distribution for the 46 310 measured drops, which is shown in Fig. 10, shows no event which cannot be explained by integral charges.

B. Stopping efficiency of the N₂ tanks

The stopping efficiency of the tanks was calculated using the same Monte Carlo simulation which was previously described in this paper. Table II shows the stopping acceptance under various assumptions. For the purpose of calculating the stopping efficiency, we assume that quarks are produced with an average transverse momentum $\langle k_T^2 \rangle^{1/2}$ of 0.5 GeV/c, have an inelastic cross section of 20 mb, strike a target of mass 1.0 GeV, and have a mass of 1 GeV. These assumptions lead to a stopping efficiency of 0.078 for charge $\frac{1}{3}$ quarks. If $\langle k_T^2 \rangle^{1/2}$ were 2.0 GeV/c, then the stopping would decrease by 35%. The effect of having an increased $\langle k_T^2 \rangle^{1/2}$ is usually insignificant except in the regions of low quark mass and high target mass where the stopping is reduced to a maximum of about $\frac{1}{3}$. The stopping using the nominal assumptions for a charged $\frac{2}{3}$ quark is 0.118 which is about 50% higher than for a $\frac{1}{3}$ charged quark.

Using the incident proton flux on the target of 4.1×10^{13} and the previously described efficiencies, we find that the upper limit is 1.2×10^{-10} charged $\frac{1}{3}$ quarks per proton interaction and 7.7×10^{-11} charged $\frac{2}{3}$ quarks per proton interaction at the 90% confidence level.

V. CONCLUSIONS

In summary, no evidence for fractional charge has been found in 800-GeV/c proton-nucleus collisions. From this experiment, upper limits using two different methods of trapping fractional charge can be determined.

TABLE II. Fraction of quarks which stop in all LN₂ tanks.

Effective target mass (GeV)	Quark-nucleus cross section (mb)	Fraction of quarks stopped with mass				
		0.5 GeV	1 GeV	2 GeV	5 GeV	10 GeV
1	5	0.011	0.005	0.012	0.010	0.018
2	5	0.007	0.004	0.019	0.020	0.015
10	5	0.014	0.025	0.033	0.052	0.045
100	5	0.010	0.024	0.036	0.067	0.065
1	20	0.056	0.078	0.100	0.150	0.179
2	20	0.042	0.086	0.137	0.163	0.173
10	20	0.045	0.084	0.174	0.191	0.249
100	20	0.035	0.078	0.143	0.239	0.280

Analyzing an irradiated target of mercury yields a limit for charged $\frac{1}{3}$ quarks of 1.2×10^{-10} quarks per proton interaction at 90% confidence limit, while a method using electrostatic attraction of quarks to a Au-plated wire results in an upper limit of 1.2×10^{-10} . The results for charged $\frac{2}{3}$ quarks are 1.1×10^{-10} and 7.7×10^{-11} , respectively.

The new method for collecting quarks by trapping them in Hg and then concentrating them by evaporation is very powerful. Highly interacting fractional particles can be collected and measured with a very high sensitivity. This technique is well suited for fixed-target experiments as essentially the whole intensity of an accelerator can be passed through the passive Hg targets.

ACKNOWLEDGMENTS

Many people have contributed to the performance of this experiment and we would like to thank them. At

Fermilab, we especially would like to thank the operations crew who provided very valuable support and D. Cossairt, A. Elwyn, and K. Krempitz who made several valuable suggestions and helped with the safety review. Also, we would like to thank J. Haley for advice on the distillation process and J. Bucher for his helpful comments and for use of his laboratory. We would also like to thank B. Chasteler, D. Hoffman, and D. Lee for assistance in measuring the γ spectrum from the distilled Hg. We had helpful discussions with F. Bauman and D. Edwards on thermal and electroconvection. Finally, we would like to acknowledge the encouragement of J. D. Bjorken whose support and assistance were vital for this project. This research was supported in part by the Director, Office of Energy Research, Office of High Energy and Nuclear Physics, Nuclear Physics Division of the U.S. Department of Energy under Contract No. DE-AC03-76SF00098, U.S. Department of Energy Contract No. DE-AC03-81ER40009, and by the National Science Foundation.

-
- ¹G. L. Shaw *et al.*, Phys. Rev. D **36**, 3533 (1987).
²M. A. Lindgren *et al.*, Phys. Rev. Lett. **51**, 1621 (1983).
³M. L. Savage *et al.*, Phys. Lett. **167B**, 481 (1986).
⁴H. S. Matis *et al.*, in *Proceedings of the XXIII International Conference on High Energy Physics*, Berkeley, California, 1986, edited by S. Loken (World Scientific, Singapore, 1987); H. S. Matis, *ibid.*, p. 627.
⁵M. Marinelli and G. Morpurgo, Phys. Lett. **137B**, 439 (1984).
⁶L. Lyons, Phys. Rep. **129**, 225 (1985).
⁷A. De Rújula, R. C. Giles, and R. L. Jaffe, Phys. Rev. D **17**, 285 (1978).
⁸R. Slansky, T. Goldman, and G. L. Shaw, Phys. Rev. Lett. **47**, 887 (1981); G. L. Shaw and R. Slansky, *ibid.* **50**, 1967 (1983).
⁹G. Zweig, Science **201**, 973 (1978).
¹⁰L. Lyons *et al.*, Z. Phys. **36**, 363 (1987).
¹¹M. Banner *et al.*, Phys. Lett. **156B**, 129 (1985).
¹²K. S. Lackner and G. Zweig, Phys. Rev. D **28**, 1671 (1983).
¹³Particle Data Group, M. Aguilar-Benitez *et al.*, Phys. Lett. **170B**, 44 (1986).
¹⁴A. Bamberger *et al.*, Phys. Lett. B **205**, 583 (1988).
¹⁵R. Slansky, Phys. Rep. **11C**, 99 (1974).
¹⁶J. R. Melcher, Phys. Fluids **10**, 325 (1967).
¹⁷L. McCarthy, Master's thesis, UCI, 1987.
¹⁸S. R. Elliott, A. A. Hahn, and M. K. Moe, Phys. Rev. Lett. **58**, 2020 (1987).